Final report of "A Detailed Study of the Physical Mechanisms Controlling CO_2-Brine Capillary Trapping in the Subsurface" (University of Arizona, DE-SC0006696)

Marcel G. Schaap
July 2016

This document is the final report of the University of Arizona's (UA) portion of the project entitled "A Detailed Study of the Physical Mechanisms Controlling CO_2-Brine Capillary Trapping in the Subsurface". This project was a collaborative effort between Oregon State University (OSU) and UA and was awarded in 2011 with an end-date of November 2014. One no-cost extension was requested and the project formally ended on November 30 2015. The experiments were conducted by OSU at the synchrotron-based x-ray micro-tomography facility at the Advanced Photon Source (APS) at Argonne National Laboratory, and the lattice Boltzmann pore scale model simulations were performed at the high-performance computing center at UA.

Executive Summary and Abstract

Carbon capture and storage (CCS) of carbon dioxide emissions generated by production or combustion of fossil fuels is a technologically viable means to reduce the build-up of CO_2 in the atmosphere and oceans. Using advantages of scale and location, CCS is particularly suitable for large point sources near ubiquitous deep saline aquifers, depleted gas reservoirs, or at production reservoirs for enhanced oil recovery (EOR). In the BES-funded research project, Oregon State University (OSU) carried out capillary trapping experiments with proxy fluids that mimic the properties of the $scCO_2$/brine system under ambient temperatures and pressures, and successfully developed a unique and novel x-ray compatible, high-pressure, elevated temperature setup to study the $scCO_2$/brine system under challenging reservoir conditions. Both methodologies were applied to a variety of porous media, including synthetic (glass bead) and geologic (Bentheimer sandstone) materials. The University of Arizona (UA) developed pore-scale lattice Boltzmann (LB) models which are able to handle the experimental conditions for proxy fluids, as well as the $scCO_2$/brine system, that are capable of simulating permeability in volumes of tens of millions of fluid elements. We reached the following summary findings (main institute indicated):

1. (OSU/UA) To understand capillary trapping in a multiphase fluid-porous medium system, the system must be analyzed from a pore-scale force balance perspective; trapping can be enhanced by manipulating wetting and nonwetting phase fluid properties.
2. (OSU) Pore-scale fluid connectivity and topology has a clear and direct effect on nonwetting phase capillary trapping efficiency.
3. (OSU) Rock type and flow regime also have a pronounced effects on capillary trapping.
4. (OSU/UA) There is a predictable relationship between NWP connectivity and NWP saturation, which allows for development of injection strategies that optimize trapping. The commonly used Land model (*Land*, 1968) does not predict amount of trapped NWP accurately.
5. (UA) There are ambiguities regarding the segmentation of large-volume gray-scale CT data into pore-volumes suitable for pore-scale modeling. Simulated permeabilities vary by three orders of magnitude and do not resemble observed values very well. Small-volume synchrotron-based CT data (such as produced by OSU) does not suffer significantly from segmentation ambiguities.
6. (UA) A standard properly parameterized Shan-Chen model LB model is useful for simulating porous media with proxy fluids as well as the $scCO_2$/brine system and produces results that are consistent with tomographic observations.
7. (UA) A LB model with fluid-interactions defined by a (modified) Peng-Robinson Equation of State is able to handle the $scCO_2$/brine system with variable solid phase wettability. This model is numerically stable at temperatures between 0 and 250 °C and pressures between 3 and 50 MPa, and produces appropriate densities above the critical point of CO_2 and exhibits three-phase separation below.

Based on above findings OSU and UA have proposed continued experimentation and pore-scale modeling of the $scCO_2$/brine system. The reported research has extensively covered capillary trapping using proxy fluids, but due to limited beam-time availability we were unable to apply our high-pressure CO_2 setup to sufficient variation in fluid properties, and initial $scCO_2$ connectivity. New data will also allow us to test, calibrate and apply our LB models to reservoir conditions

beyond those that are currently feasible experimentally. Such experiments and simulations will also allow us to provide information how suitable proxy fluids are for the $scCO_2$/brine system. We believe it would be worthwhile to pursue the following new research questions:

1. What are the fundamental differences in the physics underlying capillary trapping at ambient vs. supercritical conditions?
2. Do newly developed pore-scale trapping interactions and relationships translate to continuum scales?

A motivation for these questions was elaborated in "Capillary Trapping of Super-Critical CO_2: Linking Pore and Continuum Scales to Verify new Relationships" that was submitted to DOE-BES in 2015.

Introduction and Rationale of the Project

Carbon capture and storage (CCS) of carbon dioxide emissions generated by production or combustion of fossil fuels is a technologically viable means to reduce the build-up of CO_2 in the atmosphere and oceans. Using advantages of scale and location, CCS is particularly suitable for large point sources near ubiquitous deep saline aquifers, depleted gas reservoirs, or at production reservoirs for enhanced oil recovery (EOR). According to *Szulczewski et al.* (2012), deep, saline aquifers in the US have sufficient capacity to sequester a century's worth of CO_2 emissions from the nation's coal-fired power plants. CCS with and without EOR has been successfully demonstrated in a number of relatively small industrial and research projects around the world, with numerous projects in various stages of planning (e.g., http://sequestration.mit.edu/tools/projects/). Projects such as Sleipner (Norway) and Weyburn (Canada) have demonstrated the large-scale feasibility of CCS.

In typical CCS applications, the CO_2 is extracted from the plants' waste stream and pressurized to become a supercritical fluid ($scCO_2$) which is then injected at depths at which the supercritical state is maintained. The injected $scCO_2$ immiscibly displaces the resident brine, leaving the reservoir in a "drained" state. Because the $scCO_2$ is less dense than brine, the $scCO_2$ plume is positively buoyant and will migrate up and away from the injection point. Brine reinvades the reservoir, and thereby locks in place part of the $scCO_2$ by interfacial forces, a process called capillary trapping which results in a progressively shrinking buoyant plume. Over hundreds to thousands of years the CO_2 dissolves into the surrounding brine resulting in a negatively buoyant (sinking) phase; geochemical reactions will eventually lead to precipitation of carbonate minerals. As long as a buoyant $scCO_2$ plume is present, structural integrity of a reservoir is essential in preventing undesirable release of CO_2 to near-surface groundwater reservoirs and the atmosphere. Containment of a buoyant $scCO_2$ plume typically requires a low-permeability cap rock that is uncompromised by faults, traditional oil and gas exploration wells, or by modern extraction technologies like hydrofracking. Maximizing the fraction of CO_2 that is stored via capillary trapping and minimizing the timeframe during which this happens thus contributes significantly to the success, effectiveness, and safety of a geologic CO_2 sequestration operation. In addition to limiting the effects of a compromised cap rock, enhanced capillary trapping also significantly increases the surface area between the brine and the $scCO_2$ phases, thereby improving the, otherwise slow, kinetics of the dissolution and precipitation processes.

On a fundamental level, capillary trapping of $scCO_2$ is a *pore-scale* process that shares mechanisms that are relevant, for example in oil recovery and remediation of NAPL-contaminated aquifers. In these systems, capillary trapping has been linked to wetting and non-wetting phase (NWP) fluid properties, e.g. viscosity, density, and interfacial tension (IFT; media characteristics, including porosity, pore size distribution, wettability, pore space topology; engineering parameters, such as imbibition flow rate or alternating water and gas injection; and the initial nonwetting-saturation state of the reservoir (*Wildenschild et al.*, 2011; *Pentland et al.*, 2012; *Juanes et al.*, 2006, *Spiteri*

and Juanes, 2006). We wish to emphasize, however, that capillary trapping of $scCO_2$ differs rather significantly from trapping of oil recovery and NAPL remediation in that the goal is to *maximize* the amount of NWP storage, whereas the objective of the other applications is usually to minimize the amount of residual NWP This difference makes research into capillary trapping of $scCO_2$ unique, but also complex because $scCO_2$ phase properties (e.g. viscosity, density, and interfacial tension) exhibit large shifts with pressure and temperature which can strongly alter the trapping potential and efficiency.

The original project scope aimed to answer the following research questions:

(1) *Q1: What is the morphology of capillary trapped CO_2 at the pore scale as a function of temperature, pressure, and brine concentration (and thus interfacial tension and viscosity), and pore-space geometry under injection and subsequent imbibition?*

(2) *Q2: Is it possible to describe the capillary trapping process in numerical models using formation-dependent, but otherwise unique continuum-scale functions in permeability, capillary pressure, interfacial area, and saturation space, rather than hysteretic functions in permeability-saturation or capillary pressure-saturation space?*

(3) *Q3: How do continuum-scale relationships between P_c-S-A_{nw}–k_r developed based on pore-scale observations compare with traditional models incorporating relative permeability hysteresis (such as Land's and other models)?*

(4) *Q4: How can trapped CO_2 volume be optimized via engineered injection and sweep strategies, and for different formation types?*

The research was carried out along two tracks. OSU conducted extensive micro-scale capillary trapping experiments with proxy fluids that mimic the properties of the $scCO_2$/brine system under ambient temperatures and pressures and successfully developed a unique and novel x-ray compatible, high-pressure, elevated temperature setup to study the $scCO_2$/brine system under challenging reservoir conditions. OSU efforts and results, however, will not explicitly be reported in this document since OSU and UA received separate funding from DOE. Instead, this report will only discuss pore-scale modeling efforts conducted at UA which considered the experimental conditions for proxy fluids, as well as the $scCO_2$/brine system. We will also discuss ambiguities brought about by segmentation of noisy large-volume tomography data into pore volumes. Although such data were not explicitly acquired within the objectives of the research, we report it here because the findings are relevant for forging a link between the micro-scale explored in this project and the continuum/reservoir scale at which the CCS of $scCO_2$ takes place.

Development of lattice Boltzmann models suitable for simulating $scCO_2$ in porous media

The UA team has developed two lattice Boltzmann models that were projected to be suitable to simulate the behavior of $scCO_2$, or proxy fluids, at the pore-scale:

1) A standard Shan-Chen (SC) type model (*Shan and Chen*, 1993, 1994; *Martys and Chen*, 1996) for immiscible fluids
2) A SC-type model that is augmented with van-der Waals type equations of state (EOS) (*Yuan and Scheafer*, 2006; *Schaap and Porter*, 2013).

The advantage of the standard SC-type model is that it is simple and well-understood: it is possible to control this model for interfacial tension (*Schaap et al.*, 2007; *Porter et al.*, 2009) and contact angle (*Huang et al.*, 2007) and to a limited extent for viscosity. SC-type models are capable of simulating pressure-saturation curves (*Schaap et al.*, 2007), interfacial area, and microscale fluid patterns (*Porter et al.*, 2009) that are similar to observations. A drawback of the SC model is that it does not have an explicit notion of temperature, making this model fundamentally isothermal in nature and not able to deal with actual pressures and densities in the CO_2-brine system. The EOS-augmented model is able to realistically deal with reservoir conditions, but required significant development regarding CO_2-brine interactions, and interactions of both fluids with the solid phase.

Figure 1a shows primary drainage and secondary imbibition curves (equilibrium conditions, no flow) for a small volume of Bentheimer sandstone as computed by the standard SC-type LB model (thin lines); OSU laboratory observations from the APS are shown with thick black lines and symbols. The brine concentration in this system was 166,667 mg/L, temperature and pressure were 37 °C and 8.27MPa, respectively. The IFT for this system was 37.0 mN/m (*Bennion and Bachu*, 2008) and parameterized in the LB model according to *Schaap et al.*, (2007). The simulations show curves for three contact angles: 0, 35 and 65 degrees, each with 15 pressure-steps. Although there is obviously not an exact match between simulations and observations, we consider this comparison rather successful considering the difficulty of conducting the $scCO_2$ experiments, and the relatively small size of the volume used for the LB simulations (64^3 voxels). Both the observed data and the simulated results mimic a $scCO_2$ injection followed by invasion of brine and both show that the wetting phase saturation is less for the secondary imbibition, which for the model *potentially* indicates trapping of NWP.

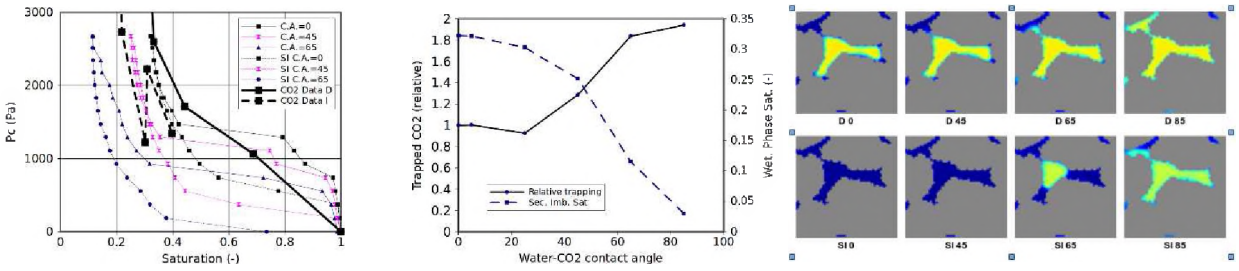

Figure 1a: Pressure saturation data (thick black lines with symbols) for $scCO_2$ in Bentheimer Sandstone and SC LB model simulation results for the same medium for three different contact angles (0, 65 and 85 degrees). **Figure 1b**: Relative NWP retention (solid line left axis) and wetting phase saturation at zero capillary pressure after secondary imbibition (dashed line, right axis). **Figure 1c**: Top row: NWP configuration after drainage (D) at an equilibrium capillary pressure of 2700 Pa for contact angles of 0 through 85°. Bottom row: corresponding fluid configurations after secondary imbibition to a capillary pressure of 0 Pa. Wetting phase (brine) is blue, NWP is green-yellow, solid phase is gray. Figures are a cross section of a 3D segment of Bentheimer sandstone.

In Figure 1b we provisionally present the amount of "trapped" $scCO_2$ as the area between the primary drainage curve and the secondary imbibition curve which is then normalized with the trapping potential at a contact angle of 0 degrees (solid line left axis). It appears that capillary trapping is approximately constant between contact angles of 0 and 35°, leading to a conclusion that small changes in solid phase wettability will likely not affect the amount of trapped NWP. Figure 1b shows that there is an *apparent* increase in trapping at larger contact angles. However, Fig 1c indicates that reduced wettability leads to an increased filling of small pores with $scCO_2$. It is likely that at increased contact angles the $scCO_2$ phase becomes increasingly connected and is therefore not trapped by snap-off mechanisms after secondary imbibition. Similar to observations by the OSU group (see *Herring et al.*, 2015b), it is likely that the topology of the NWP will determine how much will truly get trapped by capillary forces, and how much remains mobile. Additional simulations on much larger volumes of Bentheimer sandstone are currently being conducted for flow conditions that closely resemble OSU's experiments. Results regarding a comparison between observed and simulated topology a range of capillary numbers and multiple drainage and wetting cycles will be reported in (*Andersson et al.*, 2016b and *Schaap et al.*, 2016a).

The EOS-enhanced SC model aims to represent the $scCO_2$-brine system in a much more physical way by implementing and equation of state into the LB model according to *Yuan and Scheafer* (2006). We have demonstrated (*Schaap et al.*, 2012a,b) that a Peng Robinson (PR) van der Waals-type EOS leads to accurate and numerically stable simulations of pure $scCO_2$ under pressures, densities, and temperatures under reservoir conditions (Figure 2a). Simulating pure-CO_2 systems is not sufficient as the super-critical CO_2 will co-exist (and interact) with brine that is in subcritical state. Figure 2b however shows that the PR EOS is not applicable to reservoir conditions for brine: it becomes numerically unstable around 100 °C; similar instabilities were found for other published EOS types. By modifying the acentric factor in the PR equation it becomes possible to obtain numerically stable simulations under reservoir conditions (*Schaap et al.*, 2014). This model matches the liquid branch well and is suitable for at reservoir temperatures. We are still refining this extremely promising model to remove the overestimation of the vapor branch density (*Schaap*, 2016).

Recent progress has led to a complete model in which we bring together supercritical CO_2, subcritical brine and solid phase (with arbitrary wettability) by defining inter- and intra-phase force terms with adjustable parameters to obtain variable interfacial tension and contact angle. Results show that this model is stable between temperatures of approximately 0 and 250 °C and CO_2 pressures between 3 and 50 MPa and that a range of contact angles can be obtained (Figure 3). Table 1 indicates that simulated pressures, and CO_2 and brine densities are comparable to experimental values (there are some deviations near the critical point). We are currently working on a better match with experimental quantities by making further adjustments to the EOS for brine and phase interaction values (*Schaap et al.*, 2016b).

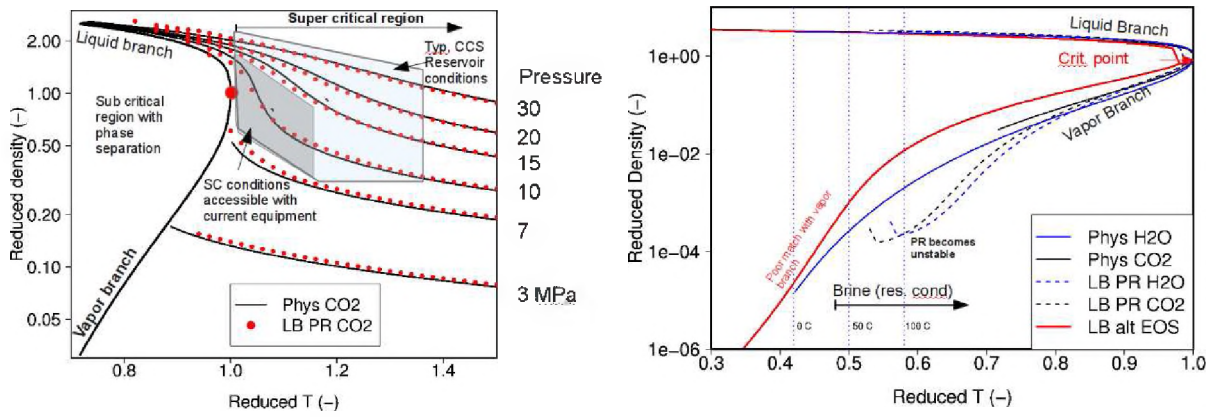

Figure 2a: pressure, density and temperature data for supercritical CO_2 (black lines) and corresponding LB simulation with the Peng-Robinson EOS model (red dots). Pressure and temperature are given in reduced units with the critical point for pure CO_2 at coordinates (1,1) coordinates, which correspond to 31 °C and 7.4 MPa. The light blue area delimits the approximate conditions relevant for reservoir-scale CCS, the gray area indicates the approximate super-critical conditions that are accessible with experiments. **Figure 2b:** subcritical densities versus reduced temperatures (solid black and blue lines for CO_2 and H_2O, respectively) and lattice Boltzmann simulations with the PR EOS (dashed black and blue lines for CO_2 and H_2O). The solid red line provides LB results with a modified PR EOS ("LB alt EOS"), which is stable under reservoir conditions for brine.

Table 2. Comparison between known experimental conditions and simulated conditions for a CO_2-brine interaction in our *uncalibrated* EOS-enhanced LB model. Simulated pressures and densities were converted to physical units, simulated interfacial tension (IFT) is given in "lattice units" as these depend on the scale at which the simulations are conducted experimental and simulated IFT are therefore not directly comparable.

Experimental conditions					Simulated conditions (uncalibrated)			
T	P (MPa)	Dens. CO_2 (kg/m^3)	Dens. brine (kg/m^3)	IFT (mN/m)	P (MPa)	Dens CO_2 (kg/m^3)	Dens. brine (kg/m^3)	IFT (lattice units)
60	7.4	169	1140	42	8.2	318	1199	0-0.56
32	13.8	820	1140	34	7.8	854	1114	0-0.54
60	13.8	551	1140	45	11.5	600.3	1147	0-0.8

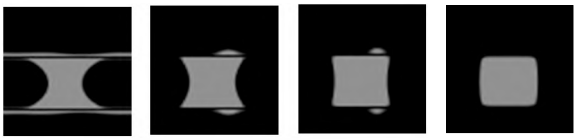

Figure 3. Brine-CO_2 LB simulations in a capillary with different solid phase potentials for brine; bine is gray, super critical CO2 is black. Note the small condensation bubbles on top and below the capillary for the second and third picture. The interfaces appear slightly non-circular due to an oblique (non-center) cut through the brine bubble.

Segmentation

During the early phases of the project a question arose how uniquely tomographic images can be converted to pore-structures suitable for pore-scale modeling. X-ray tomography relies on taking

snapshots of a porous medium from different viewing angles and a reconstruction algorithm is used to recreate a three-dimensional (3D) representation of the original porous medium. The 3D representation is a so-called "gray-scale volume" in which every 3D pixel (voxel) is assigned a value that roughly indicates the density of the material. It is necessary to convert the gray-scale volumes into "binary" images to indicate that a certain voxel corresponds to the pore-space or to a solid (or to a liquid phase, in case one or more fluids are present in the porous medium). There are many algorithms that can achieve such a binarization (or segmentation) as discussed in Iassonov et al, 2009. Unfortunately, most of these algorithms lead to rather different pore-structures -especially for gray-scale volumes with relatively large amounts of noise such as those acquired with large-volume tomographic systems (e.g. medical, industrial or bench-top x-ray tomography systems). Small-volume synchrotron-based tomography, such as used by the OSU group in this project, typically has a high signal-to-noise ratio and suffers much less for ambiguity in the imaged pore-structure (Iassonov et al., 2009). It is therefore likely that the volumes provided by OSU have pore-structures that are close to their "true" original rock samples and segmentation ambiguities are small.

However, while they can address capillary trapping, the small synchrotron-based volumes may not be large enough to fully address relative-permeability hysteresis as expressed in research questions Q3 and Q4. To this end, we investigated segmentation ambiguity in samples with a diameter of approximately 7.5 cm and a length of 20 cm (Larsen et al., 2016). As Figure 4 shows nine different segmentation algorithms (or even different parameterizations of the same algorithm, such as YASA1 through 3) can lead to radically different pore-structures and macroscopic porosity (only a 2.5 cm thick disk of the 20 cm long column is shown). Each segmentation displays somewhat different configurations of large pores and different intensities of small pores. The total porosity varies between 0.010 (4g) to 0.297 (4b). Images b and g are clearly high-porosity outliers and appear to hold most of the porosity in small pores. As a consequence, simulated permeability (Figure 5) varies by orders of magnitude, depending on the algorithm. What is worse, even though the YASA 1 and YASA 2 algorithms ("simple algorithms" developed specifically under this project) appear the least "bad", none of the algorithms does a particularly good job in representing the measured permeability (black squares) of this sample. Clearly, more research is needed to remove segmentation ambiguity from large-volume samples. Even though the research above lead to one MS thesis and one manuscript (Larsen et al., 2016) we de-emphasized large-volume pore-scale modeling pending better segmentation algorithms.

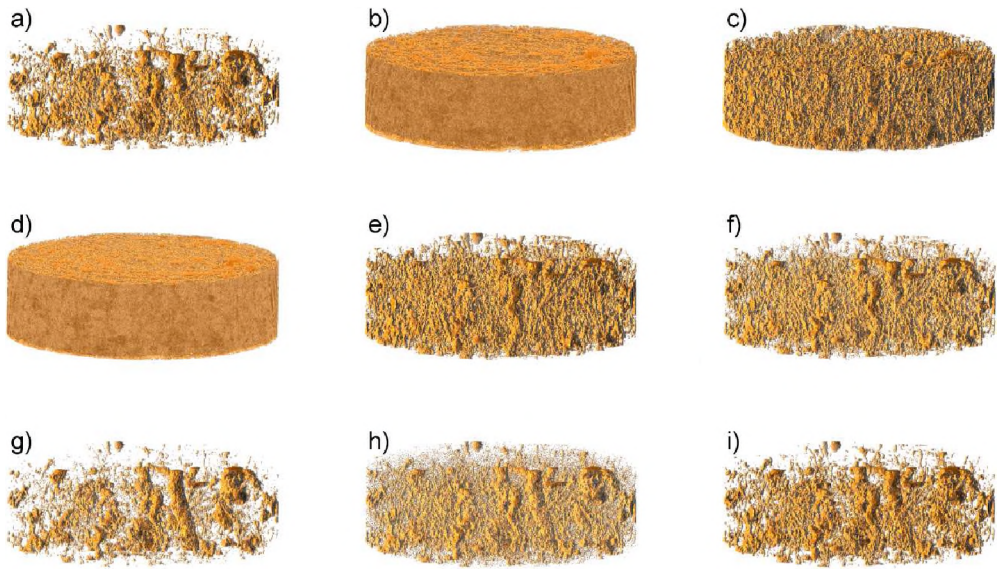

Figure 4. Three dimensional segmentations of pore-space illustrate the large variability in pore space representation between automated segmentation schemes. Porosity values are Brink 0.018 a), IK 0.297 b), KM-MRF 0.147 c), Otsu 0.238 d), Rosin 0.050 e), YASA 1 0.022 f), YASA 2 0.010 g), YASA 3 0.012 h), Yen 0.026 i).

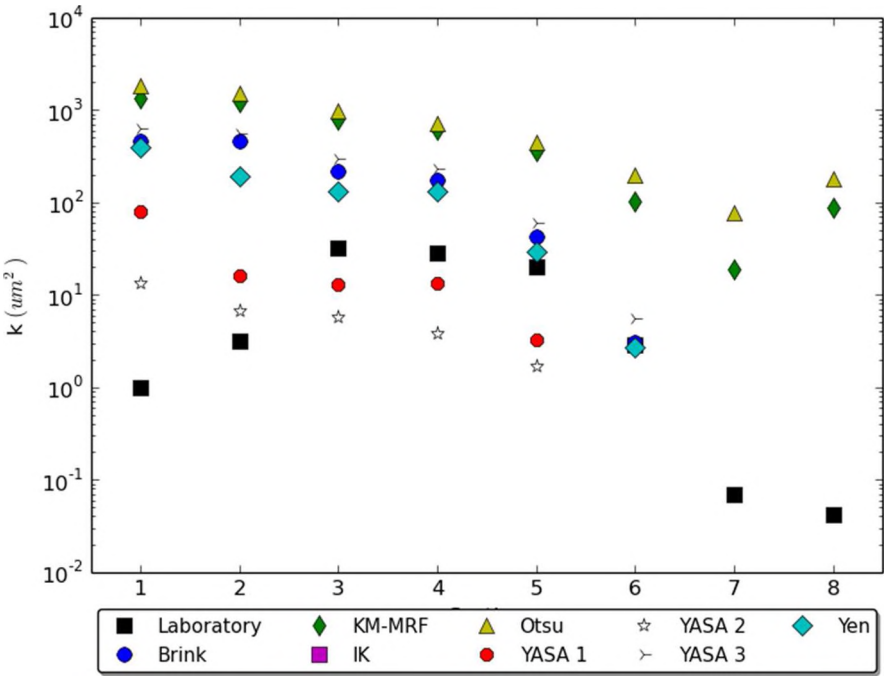

Figure 5. Lattice Boltzmann permeability models performed on eighth sized sections returned results that that range 3 orders-of-magnitude depending on the segmentation algorithm used to binarize the initial CT data. With the exception of section 6, no models produced permeability results that validate to laboratory data (Image from Larsen et al., 2016).

Conclusion and Recommendation for Further Research

The funded research reached the following main conclusions:

1. A standard properly parameterized Shan-Chen model LB model is useful for simulating porous media with proxy fluids and produces results that are consistent with tomographic observations. This model is computationally efficient and particularly suited to simulate porous media in which temperature and large density differences are irrelevant.
2. A second LB model with fluid-interactions defined by a (modified) Peng-Robinson Equation of State is able to handle the $scCO_2$/brine system with variable solid phase wettability. This model is numerically stable at temperatures between 0 and 250 °C and pressures between 3 and 50 MPa, and produces appropriate densities above the critical point of CO_2 and exhibits three-phase separation below. This model is recommended for systems with large density differences and systems where temperature has a significant influences on surface tension and wettability. This model is less computationally efficient.
3. There are ambiguities regarding the segmentation of large-volume gray-scale CT data into pore-volumes suitable for pore-scale modeling. Simulated permeabilities vary by three orders of magnitude and do not resemble observed values very well. Small-volume synchrotron-based CT data (such as produced by OSU) does not suffer significantly from segmentation ambiguities.

A list of publications (published or still in progress) follows this section. During the funded research we encountered the need for continued experimentation and simulations, especially to resolve the link between the micron-scale (5-15 μm) explored in this project and the cm to km scale at which the sequestration of $scCO_2$ actually occurs. Additional experimentation and simulation allow us to test, calibrate and apply our LB models to reservoir conditions beyond those that are currently feasible experimentally and inform the parametrization of reservoir scale models. A continuation proposal was submitted to DOE-BES in 2015.

List of publications and presentations supported by the funded research

Schaap, M.G., "Lattice Boltzmann Simulations of Pore-Scale Multi-phase Fluid Behavior", invited talk for the University of Arizona's student SIAM (Society for Industrial and Applied Mathematics) chapter, October 24 1-2pm, Mathematics building 401.

Schaap, M.G. "Lattice Boltzmann Methods for Simulating Complex Flow and Transport at the Pore-Scale" to be presented at "Workshop on Biofilm-Induced Mineralization: Modeling and Experiment", August 8-9, 2012, Montana State University, Montana.

Schaap, M.G. And D. Wildenschild, A Lattice Boltzmann Model with Realistic Equations of State for Modeling Pore-scale Effects on Capillary Trapping of CO_2 During Geological Carbon

Sequestration, AIChE, Pittsburg, Nov 1, 2012. Video of presentation: http://www.aiche.org/academy/videos/conference-presentations/lattice-boltzmann-model-realistic-equations-state-modeling-pore-scale-effects-on-capillary-trapping (2012a)

Schaap, M.G. and D. Wildenschild, Evaluation of a Lattice Boltzmann Model with Realistic Equations of State for Capillary Trapping of CO_2 at the Pore-Scale. Oral Presentation, AGU Fall meeting, December 3-7, 2012, H53M-02 (2012b)

Schaap, M.G., and M.L. Porter, Simulating Fluid Wicking Into Porous Media with the Lattice Boltzmann Method, in: Wicking in Porous Materials: Traditional and Modern Modeling Approaches, p327-353 (2013).

Schaap, M.G. Evaluation of Equations of State and Mixing Models for Simulating the Brine-CO2 System with a Lattice Boltzmann Model under Reservoir Conditions. Annual Conference of the American Geophysical Union, Dec. 8-13, 2013, San Francisco, CA, H51L-1363.

Larsen, J.D. and M.G. Schaap, 2013, Comparison of competing segmentation standards for X-ray computed topographic imaging using Lattice Boltzmann techniques. Annual Conference of the American Geophysical Union, Dec. 8-13, 2013, San Francisco, CA, H42D-04.

Larsen, J.D., M.G. Schaap, and M. Tuller, 2014. Challenges in the segmentation and analysis of X-ray Micro-CT image data, Annual Conference of the American Geophysical Union, December 15-19, H21C-0750.

Schaap. M.G., Simulation of H_2O-vapor and Brine-CO_2 in porous media with a Lattice Boltzmann Model, Annual Conference of the American Geophysical Union, December 15-19 H21C-0751, (2014)

Schaap, M.G. and D. Wildenschild, 2014. Optimizing capillary trapping of CO2 during geological carbon sequestration: Realistic Equations of State in a Lattice Boltzmann Model DOE-BES Geosciences meeting, Gaitherburg. 2015.

Larsen, J.D., 2014. Using X-ray computed tomographic imagery to estimate soil permeability with lattice Boltzmann and Kozeny-Carmen equations. MS thesis, University of Arizona.

Works still in progress:

Schaap, M.G., Andersson, L, A. L. Herring, D. Wildenschild, Pore-scale simulations of capillary trapping of supercritical CO2 after multiple drainage and imbibition cycles (In prep, journal TBD, 2016a).

Schaap, M.G., Evaluation of a lattice Boltzmann model for supercritical CO_2 in the presence of brine. (In prep, Journal TBD, 2016).

Schaap, M.G.., Andersson, L, A. L. Herring, D. Wildenschild, Pore-scale simulation of the super-critical CO2 in Bentheimer sandstone. (In prep, Journal TBD, 2016b).

Larsen, J.D., R. Kulkarni, M.G. Schaap and M. Tuller, 2016, Large scale variability observed in segmented CT fluid models of macropore soils using Lattice Boltzmann and Kozeny-Carman equation. . (In prep, Vadose Zone Journal, 2016).

References

Andersson, Herring, Schlüter, Sheppard, Wildenschild. A novel method to accurately quantify porous media aspect ratio from three-dimensional x-ray tomography images scaling with residual non-wetting phase trapping. To be submitted to Water Resources Research, (2016a).

Andersson, L, A. L. Herring, D. Wildenschild, M.G. Schaap, Simulation and experimental evaluation of pore-scale connectivity, topology and saturation levels of supercritical CO2 and brine during drainage and imbibition processes in Bentheimer sandstone. (In prep, Adv Wat. Res., 2016b).

Bennion, D.B. and S. Bachu, A Correlation of the Interfacial Tension between Supercritical-Phase CO_2 and Equilibrium Brines as a Function of Salinity, Temperature and Pressure. Proceedings of the SPE Annual Technical Conference and Exhibition, Denver, CO, Sept 21-24, 2008; SPE Paper 114479. (2008)

Herring, A. L. et al. Effect of fluid topology on residual nonwetting phase trapping: Implications for geologic CO2 sequestration. Adv. Water Resour. 62, 47–58 (2013).

Herring L. Andersson, D.L. Newell, J.W. Carey, D. Wildenschild, A. L. Pore-scale observations of supercritical CO2 drainage in Bentheimer sandstone by synchrotron x-ray imaging. Int. J. Greenh. Gas Control. International Journal of Greenhouse Gas Control 25, 93-101 (2014).

Herring, A. L., Andersson, L., Schlüter, S. & Wildenschild, D. Efficiently Engineering Pore-Scale Processes: Force Balance and Topology During Nonwetting Phase Trapping in Porous Media. Advances in Water Resour. 02/2015; 79. DOI: 10.1016/j.advwatres.2015.02.005 (2015a).

Herring, A. L., Sheppard, A. P., Andersson, L. & Wildenschild, D. Impact of Wettability Alteration on 3D Nonwetting Phase Trapping and Transport. Int. J. Greenh. Gas Control (2015b).

Herring, A., Andersson, L., D. Wildenschild. Pore-scale transport and trapping of supercritical CO2 under cyclic injection operations". (in prep for GRL), 2016a

Iassonov, P., Gebrenegus, T., Tuller, M. 2009. Segmentation of X-ray computed tomography images of porous materials: A crucial step for characterization and quantitative analysis of pore structures. Water Res. Res. 45, W09415.

Huang, H. D.T. Thorne, M.G. Schaap, M.C. Sukop, A Priori Determination of Contact Angles in Shan-and- Chen-type Multi-component Multiphase Lattice Boltzmann Models. Phys Rev E., 76, 066701 (2007).

Juanes, R., Spiteri, E. J., Orr Jr., F. M. & Blunt, M. J. Impact of relative permeability hysteresis on geological CO2 storage. Water Resour. Res. 42, W12418 (2006).

Larsen, J.D., R. Kulkarni, M.G. Schaap and M. Tuller, 2016, Large scale variability observed in segmented CT fluid models of macropore soils using Lattice Boltzmann and Kozeny-Carman equation. . (In prep, Vadose Zone Journal, 2016).

Martys, N.S. and H. Chen, Simulation of multicomponent fluids in complex three-dimensional geometries by the lattice Boltzmann method, Phys. Rev. E., 53:743-750 (1996).

Pentland, C. H., Iglauer, S., Gharbi, O., Okada, K. & Suekane, T. The influence of pore space geometry on the entrapment of carbon dioxide by capillary forces. *In*: SPE Asia Pacific Oil Gas Conf. Exhib. (Society of Petroleum Engineers, 2012).

Schaap, M. G., Porter, M. L., Christensen, B. S. B. & Wildenschild, D. Comparison of pressure-saturation characteristics derived from computed tomography and lattice Boltzmann simulations. Water Resour. Res. 43, (2007).

Schaap, M.G., and M.L. Porter, Simulating Fluid Wicking Into Porous Media with the Lattice Boltzmann Method, in: Wicking in Porous Materials: Traditional and Modern Modeling Approaches, p327-353 (2013).

Schaap. M.G., Simulation of H_2O-vapor and Brine-CO_2 in porous media with a Lattice Boltzmann Model, AGU Fall meeting, December 15-19 H21C-0751, (2014).

Schaap, M.G., Andersson, L, A. L. Herring, D. Wildenschild, Pore-scale simulations of capillary trapping of supercritical CO2 after multiple drainage and imbibition cycles (In prep, journal TBD, 2016a).

Schaap, M.G., Evaluation of a lattice Boltzmann model for supercritical CO_2 in the presence of brine. (In prep, Journal TBD, 2016b).

Schaap, M.G.., Andersson, L, A. L. Herring, D. Wildenschild, Pore-scale simulation of the super-critical CO2 in Bentheimer sandstone. (In prep, Journal TBD, 2016b).

Spiteri, E. J. & Juanes, R. Impact of relative permeability hysteresis on the numerical simulation of WAG injection. J. Pet. Sci. Eng. 50, 115–139 (2006).

Shan, X. and H. Chen, Lattice Boltzmann model for simulating flows with multiple phases and components, Phys. Rev. E. 47:1815-1819 (1993).

Shan, X. and H. Chen, Simulations of non-ideal gases and liquids-gas phase transitions by the Lattice Boltzmann Equation, Phys. Rev. E. 49:2941-2948 (1994).

Szulczewski, M. L., C. W.MacMinn, H. J.Herzog, *and* R.Juanes, Lifetime of carbon capture and storage as a climate-change mitigation technology, Proc. Natl. Acad. Sci. U. S. A., 109*(*14*)*, 5185–5189 (2012).

Wildenschild, D., Armstrong, R. T., Herring, A. L., Young, I. M. & William Carey, J. Exploring capillary trapping efficiency as a function of interfacial tension, viscosity, and flow rate. Energy Procedia 4, 4945–4952 (2011).